L3MBTL1 polycomb protein, a candidate tumor suppressor in del(20q12) myeloid disorders, is essential for genome stability

Nadia Gurvich[a], Fabiana Perna[a], Andrea Farina[b], Francesca Voza[a], Silvia Menendez[a], Jerard Hurwitz[b], and Stephen D. Nimer[a,1]

[a]Molecular Pharmacology and Chemistry Program and [b]Molecular Biology Program, Sloan-Kettering Institute, Memorial Sloan-Kettering Cancer Center, New York, NY 10065

The *l3mbtl1* gene is located on the long arm of chromosome 20 (q12), within a region commonly deleted in several myeloid malignancies. L3MBTL1 is a human homolog of the Drosophila polycomb L(3)MBT tumor suppressor protein and thus a candidate tumor suppressor in del(20q12) myeloid disorders. We used the loss-of-function approach to explore the possible tumor suppressive mechanism of L3MBTL1 and found that depletion of L3MBTL1 from human cells causes replicative stress, DNA breaks, activation of the DNA damage response, and genomic instability. L3MBTL1 interacts with Cdc45, MCM2-7 and PCNA, components of the DNA replication machinery, and is required for normal replication fork progression, suggesting that L3MBTL1 causes DNA damage, at least in part, by perturbing DNA replication. An activated DNA damage response and genomic instability are common features in tumorigenesis and a consequence of overexpression of many oncogenes. We propose that the loss of L3MBTL1 contributes to the development of 20q$^-$ hematopoietic malignancies by inducing replicative stress, DNA damage, and genomic instability.

H4K20me1/2 binding protein | chromatin reader

The *l3mbtl1* gene is located on the long arm of chromosome 20q, within a region on 20q12 commonly deleted in several myeloid malignancies, including myeloproliferative neoplasms, myelodysplastic syndromes, and acute myeloid leukemia (1). It has been proposed that the 20q12 locus contains one or more tumor suppressors, which when lost contribute to the development of these disorders. L3MBTL1 is a human homolog of the Drosophila polycomb group (PcG) protein L(3)MBT. Homozygous mutations of the Drosophila *l3mbt* gene cause malignant transformation of the adult optic neuroblasts and ganglion mother cells in the larval brain (2). Somatic, focal deletions of other human L3MBTL family members, the *l3mbtl2* and *l3mbtl3* genes, have recently been found in human medulloblastoma (3). These findings suggest that L3MBTL1 is a candidate tumor suppressor gene in myeloid malignancies associated with 20q12 deletions.

The L3MBTL1 protein contains three MBT repeats, which assume a three-bladed propeller-like architecture, as well as a Zn finger and an SPM dimerization domain (4, 5). We previously demonstrated that L3MBTL1 functions as an HDAC-independent transcriptional repressor (6) that binds preferentially to mono- and dimethylated lysines of histones via the second of its three MBT repeats (7, 8). The three MBT domains of L3MBTL1 are sufficient to compact nucleosomal arrays. This compaction requires that the nucleosome contain a mono- or dimethylated lysine 26 on histone H1b or lysine 20 on histone H4 (H4K20) (7). L3MBTL1 binds to chromatin most prominently during the S phase of the cell cycle, concomitant with the appearance of the monomethylated H4K20 (H4K20me1) mark (8), suggesting that the biological function of L3MBTL1 may be related to DNA replication.

The accurate duplication of DNA during replication is essential for maintaining genomic stability, as uncorrected errors made during this process can lead to DNA breaks, which generate mutations and/or chromosomal translocations that can promote tumorigenesis (9). DNA breaks resulting from replicative stress trigger an ATM/ATR-dependent DNA damage response (DDR), which prevents the proliferation of cells with damaged DNA by inducing either cell cycle arrest or apoptosis. An activated DDR is present in precancerous lesions from tissues of different origins, and many overexpressed oncogenes cause replicative stress and activation of the DDR. When coupled with mutations in checkpoint and/or DNA repair genes, these abnormalities can lead to cancer (10–12).

In this study we examined the function of L3MBTL1 in mammalian cells and found that L3MBTL1 interacts with several components of the DNA replication machinery. Depletion of L3MBTL1 in cells was sufficient to trigger the DDR and promote genomic instability. Thus, L3MBTL1 is essential for maintaining DNA replication, providing a mechanism for its role as a putative tumor suppressor protein.

Results

Depletion of L3MBTL1 Inhibits Cell Proliferation and Causes G2/M Arrest. To assess the role of L3MBTL1 in cell cycle regulation, we depleted L3MBTL1 mRNA and protein in U2OS cells using lentiviral vectors that expressed several shRNAs directed against its ORF. Down-regulation of L3MBTL1 mRNA and protein was achieved efficiently with three different shRNAs (≥90% knockdown; Fig. 1 *A* and *B*). The depleted cells were monitored for S phase entry by using BrdU incorporation, and we detected a marked decrease of S phase cells and the accumulation of cells in the G2/M phase (Fig. 1*C* and Fig. S1*A*). This effect was also observed in MRC5 normal diploid fibroblasts, Cal51, T98G, and K562 cells following L3MBTL1 knockdown (Fig. S1 *B–D*), demonstrating that it is not cell-type specific; it occurred in noncancerous cells as well as hematopoietic K562 cells. These findings indicate that these cell cycle effects are relevant to the myeloid compartment.

Depletion of L3MBTL1 Generates DNA Breaks. Cell cycle alterations triggered by L3MBTL1 depletion suggest that cells may be experiencing replicative stress, leading to DNA damage. To verify this hypothesis, we examined two DNA damage markers, the production of the phosphorylated histone H2A.x (γH2A.x), which localizes to sites of double-stranded DNA breaks (DSBs) (13), and the distribution of 53BP1, which is recruited to DNA within minutes following DNA damage by binding to H4K20me2 and possibly other modified histones (14). We observed an increase in both γH2A.x and 53BP1 foci following L3MBTL1 de-
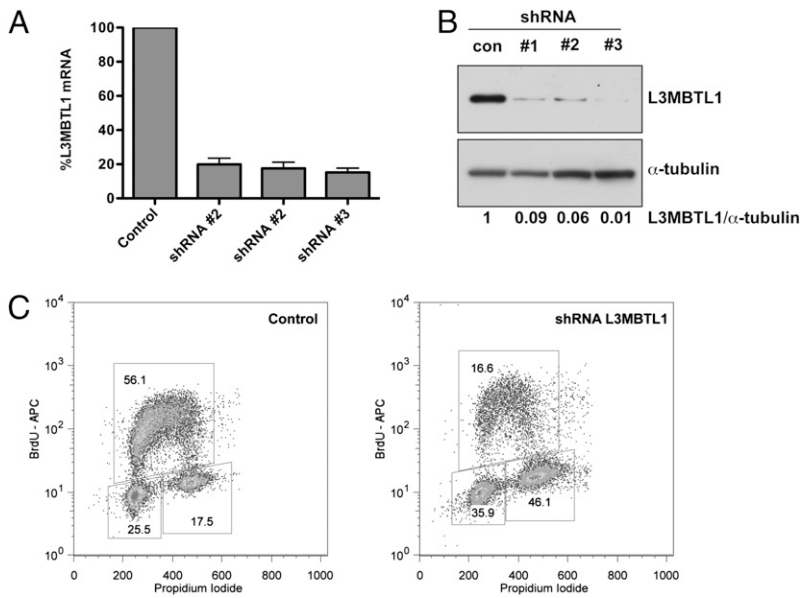
Fig. 1. L3MBTL1 depletion inhibits cell proliferation and causes G2/M arrest. U2OS cells were infected with control shRNA or one of several different lentiviral shRNAs targeting L3MBTL1. Levels of L3MBTL1 mRNA (*A*) and protein (*B*) were measured by quantitative RT-PCR and immunoblotting 48 h after infection. L3MBTL1 mRNA levels detected were adjusted for loading discrepancies using Hprt mRNA as the loading standard, and the levels of mRNA detected were plotted as a percent of the L3MBTL1 observed in U2OS cells infected with control shRNA. To quantitate depletion of L3MBTL1, the relative protein levels of L3MBTL1 were adjusted using the α-tubulin loading control and quantified relative to the protein level present in the control sample (set as 1). (*C*) U2OS cells were infected with control shRNA or with L3MBTL1 shRNA #3. After 48 h, cells were incubated with BrdU, stained with BrdU-APC antibody and propidium iodide (PI), and analyzed by flow cytometry. The distribution of BrdU (y axis) and PI (x axis) is plotted.

pletion with all three shRNAs in U2OS (Fig. 2 *A* and *B*) and in MRC5 fibroblasts (Fig. S2*A*).

We also measured the formation of DNA strand breaks in L3MBTL1-depleted cells using the comet assay, which visualizes damaged DNA on a single-cell level (15). Comet tails were detected in depleted U2OS cells (Fig. 2*C* and Fig. S2*B*), MRC5 and Cal51 cells (Fig. 2*D*), indicating DNA strand breakage. We treated MRC5 fibroblasts with varying doses of gamma irradiation to establish a range of tail moments (Fig. 2*D*) and determined that depletion of L3MBTL1 caused extensive DNA damage, similar to that induced by 5 Gy of irradiation.

Loss of L3MBTL1 Activates the DDR and Affects H4K20 Methylation Status. DNA damage triggers a checkpoint response that prevents

cells from progressing into mitosis. To explore this pathway, we first examined the phosphorylation of the ATM kinase, one hallmark of the DDR pathway (16), and detected increased phospho-ATM foci that overlapped with 53BP1 foci in L3MBTL1-depleted cells (Fig. 3*A*). We also examined whether the downstream components of the ATR/ATM-triggered DDR pathway were activated following L3MBTL1 depletion using immunoblotting to monitor changes in phosphorylation of the key components of this system, including Chk1 and Chk2. As shown in Fig. 3*B*, increased levels of phospho-Ser317-Chk1, phospho-Ser345-Chk1, and phospho-Thr68-Chk2 were detected in cells at 24, 48, and 72 h postinfection, similar to that observed in cells irradiated with 10 Gy.

Depletion of L3MBTL1 altered the activities as well as the levels of a number of proteins associated with checkpoint regu-
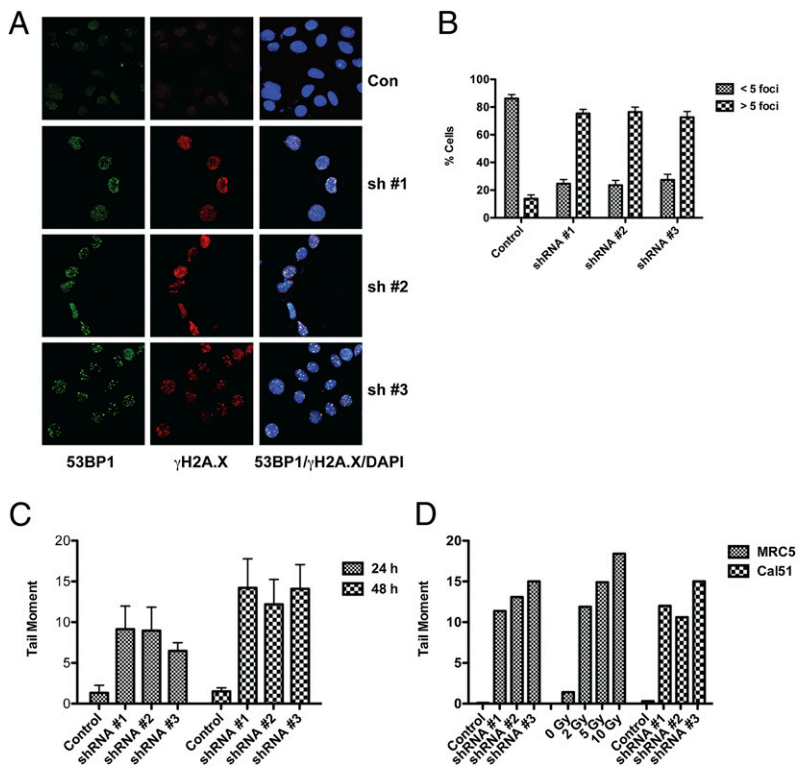

Fig. 2. Depletion of L3MBTL1 generates DNA breaks. (*A*) U2OS cells infected with one of several shRNAs against L3MBTL1 or with control shRNA were stained with antibodies against 53BP1 and γH2A.x. (*B*) DNA damage foci were quantitated in control and L3MBTL1 knockdown cells based on whether they contained more or less than five foci per cell. (*C*) The tail moment was calculated and plotted from three independent comet assays of U2OS cells treated with control shRNA or L3MBTL1 shRNA U2OS cells at 24 and 48 h after infection. (*D*) Calculated tail moments from comet assays of control and L3MBTL1-depleted MRC5 and Cal51 cells 48 h after infection are plotted. The tail moment was calculated from comet assays of control MRC5 cells vs. cells irradiated with the indicated dose of gamma irradiation and the data plotted.
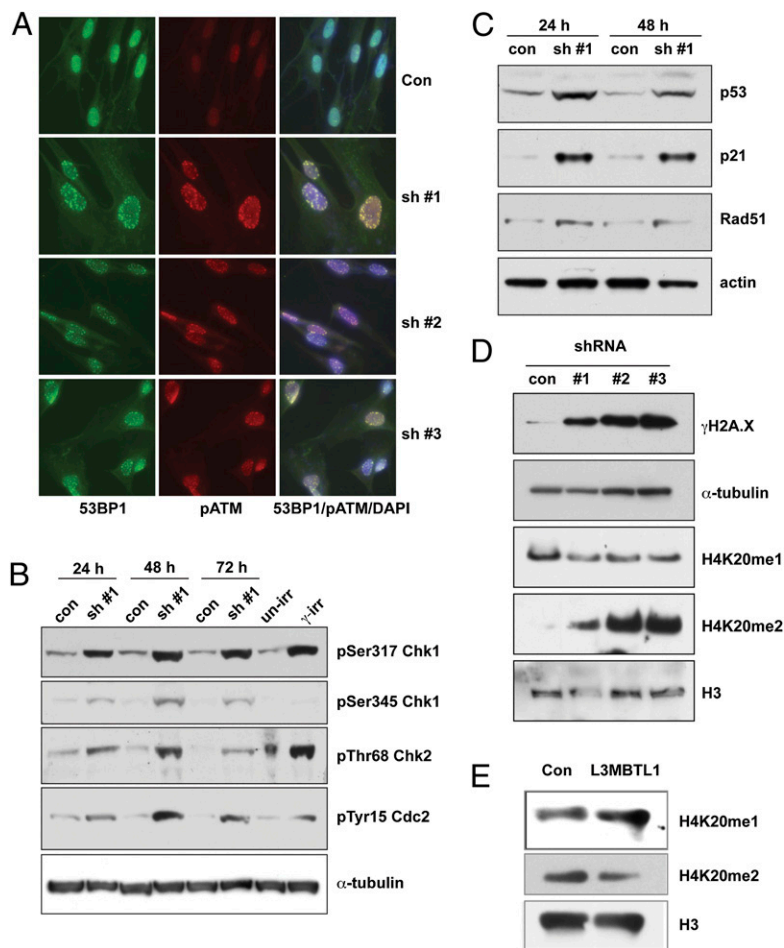
CELL BIOLOGY

Fig. 3. Depletion of L3MBTL1 activates the DDR. (*A*) Control and L3MBTL1-depleted U2OS cells were stained with antibodies against 53BP1 and phospho-ATM (pATM) 48 h postinfection. (*B*) U2OS cells infected with control or L3MBTL1 shRNAs were harvested 24, 48, and 72 h postinfection and immunoblotted with the indicated antibodies to detect activation of the DDR. Unirradiated cells (unirr) and cells harvested 1 h following 10 Gy of gamma irradiation (γ-irr) were used as negative and positive controls for activated DDR proteins. (*C*) Lysates from control and L3MBTL1-depleted U2OS cells were isolated 24 and 48 h postinfection, and the levels of Rad51, p53, p21, and actin determined by immunoblotting with the indicated antibodies. (*D*) Lysates from U2OS cells infected with three different shRNAs against L3MBTL1 were harvested at 48 h and immunoblotted with antibodies directed against γH2A.x, H4K20me1, H4K20me2, histone H3, and tubulin. (*E*) Histones were extracted from U937 cells that overexpress L3MBTL1 or that contain empty vector control and immunoblotted for H4K20me1, H4K20me2, and histone H3 (loading control).

lation and the DDR pathway (Fig. 3 *B–D*). These include: (*i*) the formation of phospho-Tyr15-Cdc2, a modification that inhibits Cdc2 kinase activity, which is required for cell cycle progression into mitosis (17) (Fig. 3*B* and Fig. S3*A*); (*ii*) the up-regulation of p21 and p53, downstream effectors of the DDR pathway, as well as Rad51, which plays a key role in double-strand break repair by homologous recombination (Fig. 3*C* and Fig. S3*B*), and (*iii*) an increase in the level of γH2A.x (Fig. 3*D* and Fig. S3*C*), in keeping with the data shown in Fig. 2. We also observed an increase in the amount of H4K20me2 (40- to 90-fold), which plays important roles in DNA replication and DNA damage recognition (18), but detected little effect on the levels of H4K20me1. Conversely, overexpression of L3MBTL1 in U937 cells that have monoallelic loss of the commonly deleted region of 20q had the opposite effect, namely, a decrease in H4K20me2 and an increase in H4K20me1 (Fig. 3*E*). Collectively, these data show that the DDR pathway is strongly activated following depletion of L3MBTL1 and suggest that changes in the level of H4K20 dimethylation could contribute to these effects.

We, and others, have found L3MBTL1 complexed with Rb/E2F proteins repressed the activation of some E2F target genes, including c-myc and Cyclin E1, two established oncogenes (7, 8, 19, 20). We tested whether these genes were up-regulated in L3MBTL1 knockdown cells, but noted no changes in their levels at 48 h following lentiviral infection with shRNAs against L3MBTL1 (Fig. S3*D*). Thus, induction of the DDR following L3MBTL1 depletion cannot be explained by the enhanced expression of c-myc or Cyclin E1.

L3MBTL1 Depletion Slows the DNA Replication Forks Movement. The presence of DNA damage and activation of the DDR suggest that

depletion of L3MBTL1 may trigger defects in DNA replication. We examined DNA replication fork progression by DNA fiber analyses. For this purpose, control and L3MBTL1-depleted cells were sequentially pulsed for 1 h each with IdU and CldU, lysed, and DNA fibers spread on slides. The fibers were labeled with antibodies to IdU and CldU and fluorescence-labeled secondary antibodies. Fibers containing green IdU fluorescent label flanked on each side with the red CldU fluorescent label represent DNA molecules formed by bidirectional movement of replication forks. Fig. 4*A* shows DNA fibers isolated from control and L3MBTL1-depleted MRC5 fibroblasts. The length of the green IdU-labeled fibers, indicating DNA replicated from origins, was shorter in depleted cells than in fibers isolated from control cells. Furthermore, the total length of red CldU- and green IdU-labeled fibers was shorter in L3MBTL1-depleted cells than in control cells, indicating slower replication fork movement. The average length of DNA fibers from L3MBTL1-depleted cells and control cells was 16.8 μM and 31.7 μM, respectively (Fig. 4*B*); 78% of the DNA fibers from L3MBTL1-depleted cells were <20 μM, whereas 33% of fibers from control cells were this length (Fig. 4*C*). Similar data were obtained using U2OS cells, indicating that this effect is not cell-type specific (Fig. 4 *D* and *E*). The average rate of fork progression in L3MBTL1-depleted cells was ~40% slower than in control cells, indicating that L3MBTL1 is required for the normal progression of DNA replication forks.

L3MBTL1 Interacts with Components of DNA Replication Machinery. Because L3MBTL1 appears to play a role in replication fork progression, we tested whether it interacted with components of the DNA replication machinery. We overexpressed HA-tagged L3MBTL1 in 293T cells, and examined its interaction with mem-
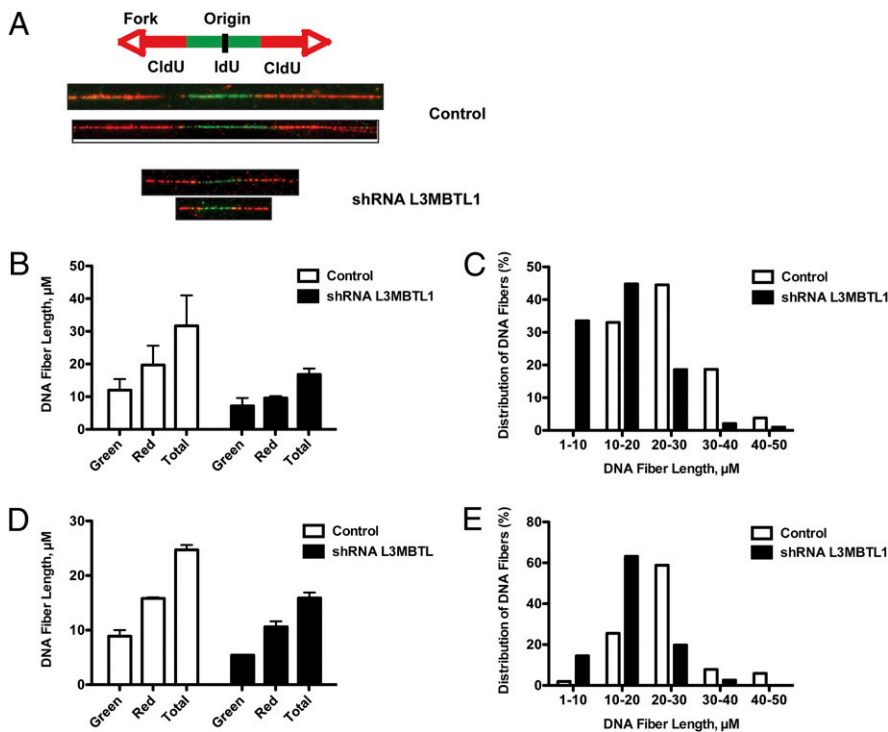
Fig. 4. Depletion of L3MBTL1 alters the progression of DNA replication forks. MRC5 and U2OS cells infected with control or L3MBTL1 shRNA were incubated for 1 h with IdU followed by 1 h incubation with CldU and then subjected to analysis of replication fork movement. (*A*) Individual replication units were visualized by immunofluorescence for incorporated halogenated nucleotides in isolated DNA fibers, as described in *Materials and Methods*. Images of fibers from MRC5 cells infected with control or L3MBTL1 shRNAs are shown. (*B*) The mean DNA fiber length from MRC5 cells infected with control or L3MBTL1 shRNA was calculated by measuring at least 100 fibers in each experiment, and the results plotted. (*C*) The data for one representative experiment with MRC5 cells are plotted as percentage of DNA fibers with each specified length. (*D*) Mean DNA fiber length for U2OS cells infected with control or L3MBTL1 shRNA was calculated by measuring at least 100 fibers in each experiment and plotted. (*E*) The data derived from an experiment using U2OS cells are plotted as percentage of replication forks with the specified DNA fiber length indicated.

bers of the MCM2-7 complex, a critical component of the putative replicative helicase. As shown in Fig. 5*A*, HA-tagged L3MBTL1 interacted with the MCM2-7 complex, and L3MBTL1 was immunoprecipitated by antibodies against MCM2 and MCM5 (Fig. 5*B*). Cdc45 and the GINS complex form a replicative helicase complex with MCM2-7 (CMG complex) (21) that travels with the replication fork (22). These findings prompted us to examine whether L3MBTL1 interacted with these components as well as other replication proteins. As shown in Fig. 5*A*, the interaction of L3MBTL1 with Cdc45 was detected, whereas an interaction with Sld5 (a subunit of the GINS complex) was not observed. Interactions with PCNA, the DNA sliding clamp required for processivity of the replicative DNA polymerases, were also noted, whereas interaction with Fen-1, an enzyme involved in DNA repair and lagging strand processing, was not observed (Fig. 5*A*). We also examined whether the levels of replication proteins were affected by depletion of L3MBTL1 in U2OS cells. As shown in Fig. S4, we did not find significant changes. Thus, L3MBTL1 interacts with a number of proteins that play roles in different stages of DNA replication, consistent with the notion that it affects replication. The mechanisms contributing to these effects remain to be investigated.

Discussion

In this study we demonstrate that depletion of L3MBTL1 induces DNA damage and slows cell cycle progression by arresting cells in the G2/M phase. L3MBTL1 interacts with components of the DNA replication machinery (MCM2-7 proteins, Cdc45, and PCNA) and is required for the normal movement of DNA replication forks. These findings suggest that L3MBTL1 influences multiple aspects of DNA replication and repair.

The methylation status of H4K20 is important in DNA replication and DDR pathways (18). SUV4-20 methyltransferase catalyzes the di- and trimethylation of H4K20, and Suv4-20 knockout mice, which can only form the H4K20me1 derivative, are more sensitive to DNA damage than wild-type mice (23). Loss of Pr-Set7, a histone methyltransferase that monomethylates lysine 20 on histone H4, induces DNA damage in human, mouse, and Drosophila cells. Pr-Set7 has also been implicated in DNA replication (24–29). We previously established that L3MBTL1 binds to mono-

and dimethylated H4K20, and interacts directly with PR-Set7. The binding of L3MBTL1 to chromatin occurs during S phase, coincidental with the appearance of H4K20me1, suggesting that it binds to the mark to exert its effects (8). Depletion of L3MBTL1 resulted in a marked increase in H4K20me2 levels (Fig. 3*D*), possibly by allowing dimethylation of H4K20 by Suv4-20 histone methyltransferase. The biological effects observed following depletion of L3MBTL1 closely parallel those resulting from the loss of Pr-Set7, suggesting that the ability of L3MBTL1 to recognize and bind to the H4K20me1 mark produced by Pr-Set7 plays an important role in maintaining genomic stability.
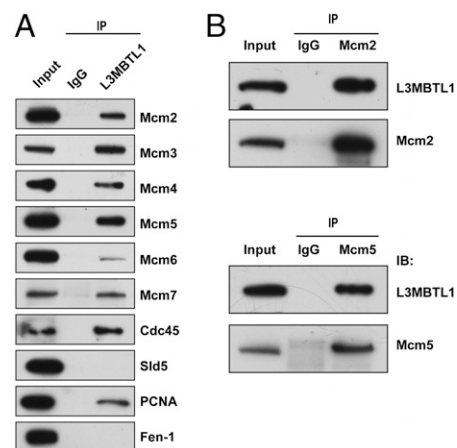
Fig. 5. L3MBTL1 interacts with components of the DNA replication machinery. (*A*) HA-L3MBTL1 was overexpressed in 293T cells, and cell lysates were immunoprecipitated and immunoblotted with the HA or rabbit IgG antibodies. (*B*) Flag-L3MBTL1 was overexpressed in 293T cells, and cell lysates were immunoprecipitated with antibodies against Mcm2, Mcm5, or rabbit IgG. Following SDS/PAGE separation, gels were immunoblotted with Flag antibody to detect L3MBTL1. The immunoprecipitation of Mcm2 and Mcm5 proteins was verified by immunoblotting with the corresponding antibodies, using rabbit IgG as a control.

At present, it is unclear how L3MBTL1 contributes to genomic stability and influences fork progression. Its role in fork progression may relate to its function in maintaining genomic stability, as L3MBTL1 depletion triggers the DDR, which leads to checkpoint activation and a halt in replication. Recently, Qin et al. (30) found that loss of L3MBTL1 in mice does not alter H4K20 methylation or result in tumor formation. Differences between the Qin et al. study (30) and ours may reflect the effects caused by the acute loss of L3MBTL1 vs. its chronic absence in the knockout mice, where functional compensation by another L3MBTL family member could occur. Furthermore, H4K20 methylation levels may be controlled differently in ES cells than in the normal, human diploid fibroblasts that we have studied. As oncogenesis is a multistep process, it seems highly likely that additional molecular events are needed to induce tumorigenesis.

Interactions between L3MBTL1 and Cdc45 and MCM2-7 suggest that L3MBTL1 may have a more direct role in DNA replication; however, further studies will be required to define the functional significance of these interactions and to determine whether the position of L3MBTL1 is within or external to nucleosomes, because nucleosome deposition occurs behind the fork on newly synthesized DNA. L3MBTL1 may also prevent the conversion of the H4K20me1 mark to H4K20me2 by Suv4-20, as we detected an increase in H4K20me2 in cells depleted of L3MBTL1. Though L3MBTL1 is degraded during mitosis (8), depletion of L3MBTL1 before the G2/M transition leads to the generation of the H4K20me2, which recruits 53BP1, thereby promoting the DDR and hindering normal replication. Normally, Suv4-20 acts during the M and G1 phases to convert H4K20me1 to H4K20me2 (31). This methylation step may occur primarily in the absence of chromatin-bound L3MBTL1. Consistent with this notion, we found that L3MBTL1 depletion slowed replication fork progression and increased the formation of 53BP1 foci. Whether removal of L3MBTL1 from the H4K20me1 mark is required for the DDR, by triggering the H4K20me2 generation and subsequent binding of 53BP1, will require further investigation.

DNA damage and genomic instability promote oncogenesis (32), and tumor samples isolated from patients at diagnosis often show constitutive activation of DNA damage signaling (10, 11). This DDR activation is most prominent in early, preinvasive stages of a diverse group of cancers. Overexpression of activated oncogenes, such as c-myc, H-Ras, Cdc25A, cyclin E1, and E2F1, in multiple cell types leads to a strong DDR activation (10, 33–35) and recapitulates the findings seen in precancerous lesions. This phenomenon is also relevant to hematopoietic malignancies, as both the PML-RARα and AML1-ETO leukemia-associated fusion proteins trigger the DDR in normal hematopoietic cells (36). Mechanistic studies implicate oncogene-induced DNA replication stress, including replication fork collapse and formation of double-stranded breaks, as the stimulus that evokes the DDR response (12), and in the case of c-myc, the induction of DNA damage was shown to result from its direct involvement in DNA replication (37). Although this response acts as a barrier against oncogene-induced transformation, acquired mutations in DNA-damage checkpoint proteins, such as p53 or ATM, could permit cells with damaged DNA to slip through the checkpoints and progress to a full-blown cancer (38).

We have shown that the depletion of L3MBTL1, a candidate tumor suppressor gene, leads to the activation of the DDR. Failure to correct DNA damage caused by the loss of L3MBTL1 could lead to genomic instability and the development of a myeloid malignancy. Indeed, we detected an increased number of specific breaks, gaps, and exchanges in metaphase chromosome spreads of L3MBTL1 knockdown cells (Fig. S5). Drosophila L3MBTL was found to be part of the Myb/E2F2/RBF complex, which has roles in both transcription and replication (18, 39), and human L3MBTL1 is also found in similar complexes (7). Moreover, Lin-61, the Caenorhabditis elegans homolog of L3MBTL1, has been implicated in maintaining genomic integrity (40, 41). These observations suggest that the role of L3MBTL1 in DNA replication and genome stability may be evolutionary conserved,

implying that the loss of L3MBTL1 contributes to the development of 20q12 hematopoietic malignancies by causing DNA damage and genomic instability.

Materials and Methods

Lentiviral and Retroviral Transduction. Lentiviral shRNA constructs were purchased from the TRC shRNA library at Thermo Scientific Open Biosystems and modified by subcloning the GFP gene instead of the puromycin gene into the pLKO.1 vector as a marker of viral integration. shRNA sequences against L3MBTL1 were gcctgcactttgatgggtatt (shRNA 1), gctggagtcatggctatgatt (shRNA 2), and gcagtcactcacaacaagaat (shRNA 3). shRNA with scrambled sequences in the same vector was used as a negative control. To produce lentiviruses, 293T cells were transfected with the shRNA constructs and helper plasmids (the envelope construct pMD2G and the packaging construct psPAX2) using the calcium phosphate method. To produce the retroviruses for the overexpression assays, Phoenix-A cells were transfected with either HA-tagged L3MBTL1 or empty MIGR1 vector construct. Lentiviruses or retroviruses were harvested by collecting and filtering supernatants 48 and 72 h after transfection, and concentrated by centrifugation at 4 °C for 2 h at 25,000 rpm in a Beckman L7-55 Ultracentrifuge. Target cells were infected with concentrated virus in the presence of 8 μg/mL polybrene by centrifugation at $450 \times g$ for 45 min.

Cell Cycle Analysis by Flow Cytometry. Cells were collected by trypsinization and fixed in 70% ethanol. They were washed with PBS, stained with 50 μg/mL propidium iodide and 0.5 μg/mL RNase A (both from Sigma-Aldrich), and analyzed by flow cytometry. For BrdU/propidium iodide staining, cells were incubated with 1 mM BrdU for 1 h and then stained with BrdU-APC antibody and propidium iodide, according to the instructions in the BrdU Flow Kit (BD Biosciences). Minimally, 10^5 cells were analyzed on the BD FACSCalibur flow cytometer, and the data were collected using BD Cell Quest Pro software and analyzed using FlowJo software (Tree Star).

Immunoblotting and Coimmunoprecipitations. U2OS cells were lysed in lysis buffer [20 mM Tris-HCl (pH 8), 0.5% Nonidet P40, 0.5% Tween 20, 1 mM EDTA, 1 mM DTT, 150 mM NaCl, 1 mM PMSF and protease inhibitor mixture (Calbiochem)], and then briefly sonicated and centrifuged. The protein concentration was measured using the Bradford assay (Bio-Rad), and equal amounts of protein were loaded on NuPage gels (Invitrogen). Protein transfer was conducted onto Immobilon-P PVDF membrane (Millipore), and the membranes immunoblotted with antibodies to the following proteins: phospho-Ser-317 Chk1, phospho-Ser354 Chk1, phospho-Thr68 Chk2, phospho-Tyr15 Cdc2, p53 (all from Cell Signaling), actin, Rad51, p21, geminin (all from Santa Cruz), α-tubulin (Sigma Aldrich), γH2A.x (Biolegend), H4K20me1, H4K20me3, H3 (all from Millipore). The anti-L3MBTL1 antibody was described previously (6). For coimmunoprecipitations, whole-cell extracts were prepared from 293T cells overexpressing HA-tagged L3MBTL1 using the same lysis buffer as above. The lysates for coimmunoprecipitations were treated with 1,000 units/mL of benzonase (Sigma Aldrich) overnight at 4 °C to degrade DNA and RNA. They were also treated with 50 μg/mL ethidium bromide to disrupt DNA-protein complexes and exclude DNA-mediated protein-protein interactions (42). The lysates were incubated overnight at 4 °C with HA-agarose beads (Roche) or normal rat IgG serum (Santa Cruz) followed by protein A agarose beads (Roche). The coimmunoprecipitates were washed four times with lysis buffer containing 250 mM NaCl before immunoblotting for the following proteins: MCM2-7 (all from Bethyl Laboratories), PCNA (Millipore), Cdc45, Fen-1, Sld5 (all from Santa Cruz). For reciprocal coimmunoprecipitation, Flag-tagged L3MBTL1 was overexpressed in 293T cells, and lysates treated as above were immunoprecipitated with antibodies against Mcm2, Mcm5, or rabbit IgG, followed by adsorption to protein A agarose beads.

Quantitative RT-PCR. U2OS cells were harvested and RNA prepared by RNeasy Plus Mini Kit (Qiagen); cDNA was synthesized using SuperScript III RT-PCR kit (Invitrogen). Quantitative PCR was conducted on an ABI7500 Real-Time PCR system using SYBR Green PCR mix (both from Applied Biosystems) and primers corresponding to the genes of interest. Primer sequences are available upon request.

Comet Assay. DNA breaks were measured using the Comet Assay Reagent Kit (Trevigen) with minor modifications. Briefly, cells embedded in low-melting point agarose on a slide were lysed, treated with alkali, and electrophoresed in 1× TBE buffer for 40 min at 1 V/cm, stained with propidium iodide, and imaged under the fluorescent microscope. To evaluate the extent of DNA damage present in each sample, the average tail moment (a product of

percent DNA in tail and tail length) of 100 cells was calculated using CometScore software (Tritek).

Immunocytochemistry. Cells were plated on coverslips, then fixed in methanol, permeabilized with 0.25% Triton-X/PBS, blocked in 2% FBS/PBS, and incubated with primary antibody for 1 h, followed by secondary antibody conjugated with a fluorescent probe for 30 min, both at room temperature. Cells were stained with DAPI, mounted onto coverslips in mounting medium (Vector Labs), and imaged on Leica Upright confocal microscope or Carl Zeiss fluorescent microscope using appropriate filters. The primary antibodies used were directed against γH2A.x (Millipore), 53BP1 (Novus Biologicals), and phospho-Ser1981 ATM (Cell Signaling), and secondary antibodies used were anti-rabbit Alexa488 and anti-mouse Alexa568 (both from Invitrogen). Quantitation of the DNA damage foci was determined by scoring foci of at least 100 cells per treatment used.

DNA Fiber Analyses. Control and L3MBTL1 knockdown U2OS and MRC5 cells were sequentially labeled with 50-μM IdU and 250-μM CldU for 1 h each. DNA fiber spreads were prepared as described previously with some modifications (43). Briefly, three aliquots of cells were resuspended in PBS at 1×10^6 cells/mL, spotted onto a microscope slide, and lysed with 15 μL of spreading buffer [0.5% SDS in 200 mM Tris-HCl (pH 7.4), 50 mM EDTA]. After 6 min, slides were tilted 15° to allow lysates to slowly move down the slide, and the resulting DNA spreads were air-dried, fixed in 3:1 methanol/acetic acid, and stored at 4 °C overnight.

The slides were then treated with 2.5 M HCl for 30 min, incubated in blocking buffer (1% BSA/0.05% Tween 20/PBS) for 1 h followed by 1 h at room temperature with 1:500 rat anti-BrdU antibody (Abcam; to detect CldU) plus 1:100 mouse anti-BrdU (BD Biosciences; to detect IdU), diluted in blocking buffer, followed by incubation for 30 min in 1:350 Alexa488-conjugated goat anti-rat antibody and 1:350 Alexa595-conjugated goat anti-mouse antibody (Invitrogen). Slides were air-dried and mounted in Prolong Gold antifade reagent (Invitrogen). Microscopy was carried out using a Zeiss LSM 5 Live Confocal microscope, and the fiber lengths were measured using Volocity software (PerkinElmer).

Metaphase Spreads. Cal51 cells were treated with Karyomax solution (Invitrogen) for 5 h and then lysed with 75 mM KCl. Cells were fixed with a 3:1 methanol/acetic acid solution, dropped onto slides, dried, and stained with DAPI. The metaphase chromosomes were imaged under the Carl Zeiss microscope and evaluated for abnormalities such as chromatid and chromosome breaks, gaps, and exchanges.

1. Dewald GW, Schad CR, Lilla VC, Jalal SM (1993) Frequency and photographs of HGM11 chromosome anomalies in bone marrow samples from 3,996 patients with malignant hematologic neoplasms. *Cancer Genet Cytogenet* 68:60–69.
2. Gateff E, Löffler T, Wismar J (1993) A temperature-sensitive brain tumor suppressor mutation of Drosophila melanogaster: Developmental studies and molecular localization of the gene. *Mech Dev* 41:15–31.
3. Northcott PA, et al. (2009) Multiple recurrent genetic events converge on control of histone lysine methylation in medulloblastoma. *Nat Genet* 41:465–472.
4. Wang WK, et al. (2003) Malignant brain tumor repeats: A three-leaved propeller architecture with ligand/peptide binding pockets. *Structure* 11:775–789.
5. Min J, et al. (2007) L3MBTL1 recognition of mono- and dimethylated histones. *Nat Struct Mol Biol* 14:1229–1230.
6. Boccuni P, MacGrogan D, Scandura JM, Nimer SD (2003) The human L(3)MBT polycomb group protein is a transcriptional repressor and interacts physically and functionally with TEL (ETV6). *J Biol Chem* 278:15412–15420.
7. Trojer P, et al. (2007) L3MBTL1, a histone-methylation-dependent chromatin lock. *Cell* 129:915–928.
8. Kalakonda N, et al. (2008) Histone H4 lysine 20 monomethylation promotes transcriptional repression by L3MBTL1. *Oncogene* 27:4293–4304.
9. Paulsen RD, Cimprich KA (2007) The ATR pathway: Fine-tuning the fork. *DNA Repair (Amst)* 6:953–966.
10. Bartkova J, et al. (2005) DNA damage response as a candidate anti-cancer barrier in early human tumorigenesis. *Nature* 434:864–870.
11. Gorgoulis VG, et al. (2005) Activation of the DNA damage checkpoint and genomic instability in human precancerous lesions. *Nature* 434:907–913.
12. Halazonetis TD, Gorgoulis VG, Bartek J (2008) An oncogene-induced DNA damage model for cancer development. *Science* 319:1352–1355.
13. Foster ER, Downs JA (2005) Histone H2A phosphorylation in DNA double-strand break repair. *FEBS J* 272:3231–3240.
14. Schultz LB, Chehab NH, Malikzay A, Halazonetis TD (2000) p53 binding protein 1 (53BP1) is an early participant in the cellular response to DNA double-strand breaks. *J Cell Biol* 151:1381–1390.
15. Liao W, McNutt MA, Zhu WG (2009) The comet assay: A sensitive method for detecting DNA damage in individual cells. *Methods* 48:46–53.
16. Shiloh Y (2003) ATM and related protein kinases: Safeguarding genome integrity. *Nat Rev Cancer* 3:155–168.
17. Norbury C, Blow J, Nurse P (1991) Regulatory phosphorylation of the p34cdc2 protein kinase in vertebrates. *EMBO J* 10:3321–3329.
18. Yang H, Mizzen CA (2009) The multiple facets of histone H4-lysine 20 methylation. *Biochem Cell Biol* 87:151–161.
19. Lewis PW, et al. (2004) Identification of a Drosophila Myb-E2F2/RBF transcriptional repressor complex. *Genes Dev* 18:2929–2940.
20. Lu J, Ruhf ML, Perrimon N, Leder P (2007) A genome-wide RNA interference screen identifies putative chromatin regulators essential for E2F repression. *Proc Natl Acad Sci USA* 104:9381–9386.
21. Moyer SE, Lewis PW, Botchan MR (2006) Isolation of the Cdc45/Mcm2-7/GINS (CMG) complex, a candidate for the eukaryotic DNA replication fork helicase. *Proc Natl Acad Sci USA* 103:10236–10241.
22. Gambus A, et al. (2006) GINS maintains association of Cdc45 with MCM in replisome progression complexes at eukaryotic DNA replication forks. *Nat Cell Biol* 8:358–366.
23. Schotta G, et al. (2008) A chromatin-wide transition to H4K20 monomethylation impairs genome integrity and programmed DNA rearrangements in the mouse. *Genes Dev* 22:2048–2061.
24. Jørgensen S, et al. (2007) The histone methyltransferase SET8 is required for S-phase progression. *J Cell Biol* 179:1337–1345.
25. Tardat M, Murr R, Herceg Z, Sardet C, Julien E (2007) PR-Set7-dependent lysine methylation ensures genome replication and stability through S phase. *J Cell Biol* 179:1413–1426.
26. Sakaguchi A, Steward R (2007) Aberrant monomethylation of histone H4 lysine 20 activates the DNA damage checkpoint in Drosophila melanogaster. *J Cell Biol* 176:155–162.
27. Oda H, et al. (2009) Monomethylation of histone H4-lysine 20 is involved in chromosome structure and stability and is essential for mouse development. *Mol Cell Biol* 29:2278–2295.
28. Huen MS, Sy SM, van Deursen JM, Chen J (2008) Direct interaction between SET8 and proliferating cell nuclear antigen couples H4-K20 methylation with DNA replication. *J Biol Chem* 283:11073–11077.
29. Houston SI, et al. (2008) Catalytic function of the PR-Set7 histone H4 lysine 20 monomethyltransferase is essential for mitotic entry and genomic stability. *J Biol Chem* 283:19478–19488.
30. Qin J, et al. (2010) Chromatin protein L3MBTL1 is dispensable for development and tumor suppression in mice. *J Biol Chem* 285:27767–27775.
31. Pesavento JJ, Yang H, Kelleher NL, Mizzen CA (2008) Certain and progressive methylation of histone H4 at lysine 20 during the cell cycle. *Mol Cell Biol* 28:468–486.
32. Luo J, Solimini NL, Elledge SJ (2009) Principles of cancer therapy: Oncogene and non-oncogene addiction. *Cell* 136:823–837.
33. Denko NC, Giaccia AJ, Stringer JR, Stambrook PJ (1994) The human Ha-ras oncogene induces genomic instability in murine fibroblasts within one cell cycle. *Proc Natl Acad Sci USA* 91:5124–5128.
34. Bartkova J, et al. (2006) Oncogene-induced senescence is part of the tumorigenesis barrier imposed by DNA damage checkpoints. *Nature* 444:633–637.
35. Di Micco R, et al. (2006) Oncogene-induced senescence is a DNA damage response triggered by DNA hyper-replication. *Nature* 444:638–642.
36. Viale A, et al. (2009) Cell-cycle restriction limits DNA damage and maintains self-renewal of leukaemia stem cells. *Nature* 457:51–56.
37. Dominguez-Sola D, et al. (2007) Non-transcriptional control of DNA replication by c-Myc. *Nature* 448:445–451.
38. Bartek J, Bartkova J, Lukas J (2007) DNA damage signalling guards against activated oncogenes and tumour progression. *Oncogene* 26:7773–7779.
39. Beall EL, et al. (2002) Role for a Drosophila Myb-containing protein complex in site-specific DNA replication. *Nature* 420:833–837.
40. Pothof J, et al. (2003) Identification of genes that protect the C. elegans genome against mutations by genome-wide RNAi. *Genes Dev* 17:443–448.
41. Harrison MM, Lu X, Horvitz HR (2007) LIN-61, one of two Caenorhabditis elegans malignant-brain-tumor-repeat-containing proteins, acts with the DRM and NuRD-like protein complexes in vulval development but not in certain other biological processes. *Genetics* 176:255–271.
42. Méndez J, Stillman B (2000) Chromatin association of human origin recognition complex, cdc6, and minichromosome maintenance proteins during the cell cycle: Assembly of prereplication complexes in late mitosis. *Mol Cell Biol* 20:8602–8612.
43. Jackson DA, Pombo A (1998) Replicon clusters are stable units of chromosome structure: Evidence that nuclear organization contributes to the efficient activation and propagation of S phase in human cells. *J Cell Biol* 140:1285–1295.

CELL BIOLOGY